PCCP

Accepted Manuscript

This article can be cited before page numbers have been issued, to do this please use: A. al Muslim, D. Ayyash, S. S. Gujral, G. M. Mekhail, P. R. P. Nekkar and S. Wettig, *Phys. Chem. Chem. Phys.*, 2016, DOI: 10.1039/C6CP07688B.

View Article Online
DOI: 10.1039/C6CP07688B

Journal Name

ARTICLE

Synthesis and Characterization of Asymmetrical Gemini Surfactants

Received 00th January 20xx,
Accepted 00th January 20xx

DOI: 10.1039/x0xx00000x

www.rsc.org/

Aula Al Muslim,[a,b] Dana Ayyash,[a] Sarbjeet Singh Gujral[a], George M. Mekhail[a,c], Praveen P. N. Rao[a], and Shawn D. Wettig[a,b,†]

The effect of variation in the length of surfactant hydrocarbon tail groups was tested in a series of dissymmetric gemini surfactants (*N^1-alkyl N^1,N^1,N^3,N^3- tetramethyl-N^3-(6-pyren-6yl)-hexyl) propane-1,3-diammonium dibromide*) designated as $C_mC_3C_nBr$, with m=hexyl pyrene, and n= 8,12,14,16, and 18. The aggregation properties of these surfactants have been investigated by means of ^{1}HNMR, fluorescence sepctroscopy, surface tension and electrical conductivity measurements. The critical micelle concentration (CMC) was determined using surface tension and confirmed using the specific conductance method. Krafft temperatures and the degree of micelle ionization (α) were obtained from specific conductance measurements . With an increase of the dissymmetry (m/n) ratio, the CMC decreased linearly and an increase in the Krafft temperatures was observed for all of the gemini surfactants. α values for the dissymmetric GS were higher than those of the m-3-m counterparts, which may be attributed to enhanced micelle-micelle interactions that arise from increased hydrophobicity of the hydrocarbon chains. The introduction of the bulky pyrenyl tail group resulted in much lower CMC values compared to their symmetrical counterparts afftecting the packing of these surfactants at the air/ water interface, which resulted in high-ordered structures (lamellar and inverted micelles). This in turn affected the thermodymanic parameters of the micellization.

Introduction

Gemini surfactants are amphiphilic compounds composed of two hydrophilic heads and two hydrophobic tails, which are connected by a spacer group at the head area or near it. In aqueous solution, amphiphilic molecules associate to minimize the exposure of the hydrophobic components to the water phase forming hydrophobic micro-domains (known as micelles) which are stabilized in solution by the hydrophilic components. Gemini surfactants are attractive compounds which can be utilized in various applications, including soil remediation, soap and pigment industries, drug entrapment, and recently, in gene delivery.[1] Gemini surfactants possess unique characteristics that make them of substantial interest in the aforementioned applications. One of the most important properties of gemini surfactants is their ability to form aggregates of various morphologies in aqueous solutions, which increases their potential utility for drug entrapment and gene delivery applications.[2, 3] Their low critical micelle concentration (CMC) is two to three orders of magnitude lower than the conventional surfactants[4], which can lead to lower surfactant concentration in drug and gene delivery applications.

The most well- studied category of GSs are the N,N-bis[(dimethyl alkyl)-α,ω-alkanediammonium dibromide] surfactants, known generally as m-s-m type gemini surfactants, where m represents the carbon chain length of the alkyl tail and s the number of carbon atoms in the polymethylene spacer.[5] The effect of the alkyl tail chains on the physiochemical properties of the symmetrical gemini surfactants has been the focus of numerous studies[6], but little work has been carried out to examine the self-assembly and micellization of the dissymmetric gemini surfactants.[7] The micellization of dissymmetric m-s-n surfactants in solution is highly governed by the total hydrophobic chain length (m + n) and the extent of dissymmetry (m-n).[8] With an increase in the m/n ratio of asymmetry, the CMC is observed to decrease linearly with the degree of micelle ionization (α) being only slightly affected and the Gibbs free energy of micellization becoming more negative, with a correspondingly more negative enthalpy.[9]

[a] School of Pharmacy, University of Waterloo, 200 University Ave. W., Waterloo ON N2L 3G1, Canada.
[b] Waterloo Institute for Nanotechnology, University of Waterloo, 200 University Ave. W., Waterloo ON N2L 3G1, Canada.
[c] Department of Pharmaceutics and Industrial Pharmacy, Faculty of Pharmacy, Ain Shams University, Khalifa El-Maamon Street, Abbasiya Square, Cairo 11566, Egypt
† Corresponding author: wettig@uwaterloo.ca; +1-519-888-4567 Ext. 21303.
Electronic Supplementary Information (ESI) available: [details of any supplementary information available should be included here]. See DOI: 10.1039/x0xx00000x

View Article Online
DOI: 10.1039/C6CP07688B

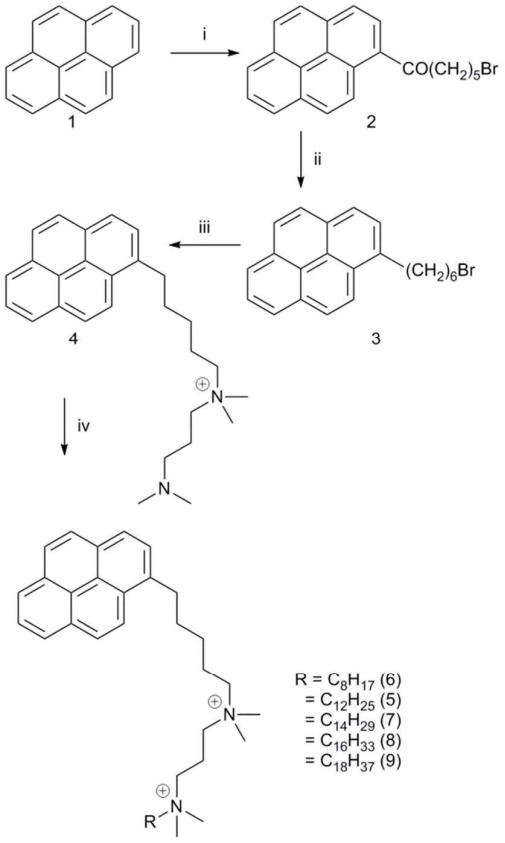

Scheme 1:. Synthesis of Pyr-3-m surfactants. Reagents and conditions: (i) Br $(CH_2)_5COCl$, $AlCl_3$, CH_2Cl_2, -78C°, (ii) Et_3SiH, TFA, 0C°, (iii) *N,N,N′,N′*-tetramethylpropane- diamine, CH_3CN, (iv) 1-bromooctane, 1-bromododecane,1-bromotetradecane, 1-bromohexadecane, 1-bromooctadecane with m= hexyl pyrene, and m= 8, 12, 14, 16, and 18

In this current study, we aimed to synthesize and characterize two groups of dissymmetric gemini surfactants, referred to as m-s-n. The first group consisted of m-s-n surfactants with one hexyl pyrene tail and one alkyl tail (n= 8,12,14,16 and 18). Meanwhile the second m-s-n had two alkyl tails, where: m=12 and n=14, 16, and 18. We also aimed to investigate the physiochemical properties of these GSs using surface tension, and specific conductance to determine the critical micelle concentration, surface tension. Krafft temperature, Krafft point, head group area, packing parameter, degree of micelle ionization, and thermodynamic properties of micellization.

Materials and Methods

Materials

Pyrene, 6-bromohexanoyl chloride, anhydrous aluminum chloride, triethylsilane, trifluoroacetic acid, *N,N,N′,N′-tetramethyl propanediamine*, 1-bromododecane, 1-bromotetradecane, 1-bromohexadecane, 1-bromooctane, 1-bromooctadecane, were purchased from Aldrich Inc. All solutions were prepared using ultrapure water obtained from a Millipore Milli-Q filtration system. The synthesis of the surfactants, as well as intermediates, are described in detail in the following sections. The general reaction schemes are shown in Schemes 1 and 2.

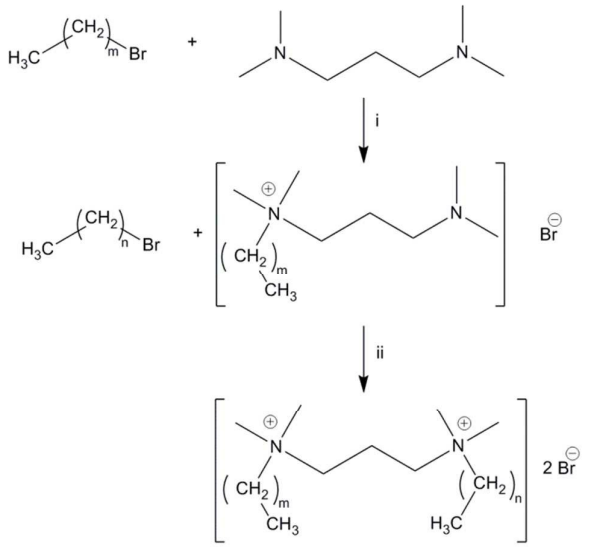

Scheme 2: Synthesis of 12-3-n surfactants. Reagents and Conditions: (i) CH_3CN, 89C°, (ii):CH_3CN, 1-bromotetradecane, 1-bromohexadecane and 1-bromooctadecane, with n=12, and n= 14, 16, and 18

5-Bromohexane-1-pyrene ketone(2): The synthesis was carried out as described by Wang et al.[10] Pyrene (49.4 mmol) and $AlCl_3$ (60mmol) were dissolved in 80 mL of precooled CH_2Cl_2 (-78C°). Another 80 mL of CH_2Cl_2 containing 6-bromohexanoyl chloride (24.7 mmol) was added in a drop wise fashion to the mixture and the reaction continued for 3h at -78°C. The reaction was quenched with 1M HCl and neutralized with $NaHCO_3$, and washed using a saturated aqueous solution of NaCl. The oil layer was separated and dried with anhydrous Na_2SO_4 overnight. The excess solvent was removed via rotary evaporation and gave a yellow/greenish paste that was further purified by soxhlet extraction with pentane to yield a light yellow solid (yield= 80%). ^{1}HNMR ($CDCl_3$, 300MHz) δ(ppm): 8.84 (d, 1H, pyr-H), 8.31-8.01 (m, 8H, pyr-H), 3.45 (t, 2H, CH_2Br), 3.24 (t, 2H, α-CH_2), 1.98-1.84 (m, 4H, β-CH_2 and δ-CH_2), 1.65-1.55 (m, 2H, γ-CH_2).

6-(1-Pyrene bromohexane)(3): This reaction was carried out as previously reported.[11] Trifluoroacetic acid (15 mL) and 5-bromohexane-1-pyrene ketone (6.0 mmol) were dissolved in 65mL CH_2Cl_2 which was precooled to 0°C. 2.7 mL of triethylsilane was added, dropwise, to the mixture and stirred under an Argon atmosphere for three days. The reaction was neutralized using saturated aqueous $NaHCO_3$ and the organic layer was separated and dried overnight with anhydrous Na_2SO_4. The product was then purified using soxhlet extraction with pentane (100%). A final yield of 92% was produced. ^{1}HNMR ($CDCl_3$, 300MHz) δ(ppm): 8.27-7.83 (m, 9H, pyr-H).

View Article Online
DOI: 10.1039/C6CP07688B

3.41-3.30 (superimposed triplets, 4H-α-CH_2, pyr-CH_2), 1.90-1.81 (4H, β-CH_2, ε-CH_2), 1.514-1.42(m, 4H, γ-CH_2, δ-CH_2).

Pyr-3: (*N*-(3-dimethylaminopropyl)-*N,N*-dimethyl-6-(pyren-6-yl)-hexane-1-ammonium bromide)(4): 6-(1-pyrene)-bromohexane (10.4 mmol) and *N,N,N′,N′*- tetramethylpropane diamine (13.2 mmol) were dissolved in 50 mL of anhydrous acetonitrile and the mixture was stirred at 45˚C for three days. The solvent was removed using rotary evaporation leaving a light yellowish precipitate. This crude product was further recrystallized from acetonitrile to yield an off-white solid (40%). ^{1}HNMR ($CDCl_3$, 300MHz) δ(ppm): 8.20-7.78 (m, 9H, pyr-H), 3.43 (m, 2H-N^+-CH_2), 3.40-3.16 (m, 4H, py-CH_2 & CH_2-N^+), 3.05 (S, 6H, N^+-$(CH_3)_2$), 2.36 (broad, 2H, CH_2-N), 2.23 (S, 6H, $N(CH_3)_2$), 1.87-1.51 (m, 10H, $(CH_2)_4$ & β-CH_2.

Pyrene-3-12: (N^1-dodecyl-N^1,N^1,N^3,N^3-tetramethyl-N^3-(6-pyren-6yl)-hexyl) propane-1,3-diammonium dibromide(5): Pyrene-3 (4 mmol) and 1-bromododecane (9.0 mmol) were added to 40 mL of anhydrous acetonitrile and the mixture was stirred at 45C˚ for two days. The solvent was removed using rotary evaporation and the product was recrystallized from a mixture of acetone and ethyl acetate (1:2), and dried overnight under vacuum with a yield of 1.5 g (50%). ^{1}HNMR ($CDCl_3$) δ(ppm): 8.23.-7.78 (m, 9H, pyr-H), 3.77-3.7 (4H, t, N^+-CH_2 (spacer)), 3.33-3.31(6H, m, pyr-CH_2 & N^+-CH_2)- chain)), 3.20 (6H, S, N^+-$(CH_3)_2$- pyr-side), 1.98(6H, S, N^+-$(CH_3)_2$- dodecyl chain), 1.66(2H, m, CH_2, spacer), 1.38-1.22(28H, m, CH_2), 0.87(3H, t, C-CH_3).

Pyrene-3-8: (N^1-octyl-N^1,N^1,N^3,N^3-tetramethyl-N^3-(6-pyren-6yl)-hexyl)-propane-1,3-diammonium dibromide)(6): Pyrene-3 (4 mmol) and 1-bromooctane (9 mmol) were treated as above for pyrene-3-12 with a yield of 1 g (35%). ^{1}HNMR ($CDCl_3$) δ(ppm): 8.17-7.80 (m, 9H, pyr-H), 3.77 (4H, t, N^+-CH_2 (spacer)), 3.61 (m, 6H, pyr-CH_2, N^+-CH_2-chain), 3.144 (S,6H, N^+-$(CH_3)_2$-pyrenyl side), 2.73 (S, 6H, N^+-CH_2- octyl side), 1.87 (m, 2H, CH_2-spacer), 1.80-1.23 (m, 20H, octyl chain & hexyl at pyrene-end), 0.89 (t, 3H, CH_3- octyl chain).

Pyrene-3-14: (N^1-tetradecyl-N^1,N^1,N^3,N^3-tetramethyl-N^3-(6-pyren-6yl)-hexyl)-propane-1,3-diammonium dibromide)(7): Pyrene-3 (4 mmol) and 1-bromotetradecane (9 mmol) were treated as above for pyrene-3-12 with a yield of 1.5 g (50%). ^{1}HNMR ($CDCl_3$) δ(ppm): 8.19-7.79 (m, 9H, pyr-H), 3.72-3.57 (t, 4H, N^+-CH_2, spacer), 3.31-3.31 (m, 6H, pyr-H & chain-H), 3.11 (S, 6H, N^+-$(CH_3)_2$), 2.55 (S, 6H, N^+-$(CH_3)_2$), 2.11 (m, 2H- CH_2-spacer), 1.79-1.19 (m, 32H, tetradecyl chain and hexyl chain), 0.85 (t, 3H, CH_3-chain).

Pyrene-3-16: (N^1-hexadecyl-N^1,N^1,N^3,N^3-tetramethyl-N^3-(6-pyren-6yl)-hexyl)-propane-1,3-diammonium dibromide)(8): Pyrene-3 (4 mmol) and 1-bromohexadecane (9 mmol) were treated as above for pyrene-3-12 with a yield of 1.5 g (50%). ^{1}HNMR ($CDCl_3$) δ(ppm): 8.23-7.80 (m, 9H, pyr-H), 3.59 (t, 4H, spacer), 3.38-3.30 (m, 6H, pyr-H & chain-H), 3.11 (S, 6H, N^+-$(CH_3)_2$), 2.59 (S, 6H, N^+-$(CH_3)_2$), 2.15 (m, 2H- CH_2-spacer), 1.83-1.21 (m, 36H, hexadecyl chain and hexyl chain), 0.85 (t, 3H, CH_3-chain).

Pyrene-3-18: (N^1-octadecyl-N^1,N^1,N^3,N^3-tetramethyl-N^3-(6-pyren-6yl)-hexyl)-propane-1,3-diammonium dibromide)(9): Pyrene-3 (4 mmol) and 1-bromohexadecane (9 mmol) were treated as above for pyrene-3-12 with a yield of 1 g (35%). ^{1}HNMR ($CDCl_3$) δ(ppm): 8.24-7.80 (m, 9H, pyr-H), 3.72 (t, 4H, spacer), 3.41-3.22 (m, 6H, pyr-H & chain-H), 3.18 (S, 6H, N^+-$(CH_3)_2$), 2.70 (S, 6H, N^+-$(CH_3)_2$), 2.11 (m, 2H- CH_2-spacer), 1.79-1.21 (m, 36H, octadecyl chain and hexyl chain), 0.84 (t, 3H, CH_3-chain).

12-3-14: (*N*-dodecyl-*N*′-tetradecyl-1,3-propanediammonium dibromide): 1-bromododecane (8.02 mmol) and *N,N,N`,N`-tetramethylpropane diamine* (1.34 mL) were added to 40 mL of anhydrous acetonitrile and the mixture was stirred for 24h at 89C°. The product was recrystallized and 1-bromotetradecane (2.39ml) was then added to the 12-3 intermediate and the reaction was continued at 89C° for another 24h. The product was recrystallized from hot acetonitrile and ethyl acetate (1:1ratio), and dried in vacuum for two days to give a yield of (1g, 50%). ^{1}HNMR ($CDCl_3$) δ(ppm): 3.88-3.83 (t,2H, α (CH_2)-spacer, 3.50-3.46 (t,2H, γ-(CH_2)-spacer, 3.38(s,12H, $(CH_3)_4$), 3.02-2.97(m, 4H, $(CH_2)_2$), 1.82-1.78 (m, 4H, $(CH_2)_2$), 1.34-1.23(m, 40H, $(CH_2)_{20}$ & ß-CH_2-spacer), 0.88-0.83(t, $(CH_3)_2$).

12-3-16: (*N*-dodcyl-*N′*-hexadecyl-1,3-propanediammonium dibromide): 1-bromododecane and *N,N,N`,N`*-tetramethyl-propane diamine were mixed in the same way as for 12-3-14 (above) to produce the 12-3 intermediate and then 1-bromohexadecane was also added in the same manner and conditions. A yield of 0.8g (35%) was obtained. ^{1}HNMR ($CDCl_3$) δ(ppm): 3.88-3.83 (t,2H, α (CH_2)-spacer, 3.50-3.46 (t,2H, γ-(CH_2)-spacer, 3.38(s,12H, $(CH_3)_4$), 3.02-2.97(m, 4H, $(CH_2)_2$), 1.82-1.78 (m, 4H, $(CH_2)_2$),1.34-1.28(m, 4H-$(CH_2)_2$, 1.25-1.23(m, 42H, $(CH_2)_{21}$ and ß-CH_2-spacer), 0.88-0.83(t, $(CH_3)_2$).

12-3-18: (*N*-dodecyl-*N′*-octadecyl-1,3-propanediammonium dibromide): 1-bromododecane and *N,N,N`,N`-tetramethyl-propane diamine* were mixed in the same way as for 12-3-14 (above) to produce the 12-3 intermediate and then 1-bromohexadecane was also added in the same manner and conditions. A yield of 1g, (50%) was obtained. ^{1}HNMR ($CDCl_3$) δ(ppm): 3.88-3.83 (t,2H, α (CH_2)-spacer, 3.50-3.46 (t,2H, γ-(CH_2)-spacer, 3.38(s,12H, $(CH_3)_4$), 3.02-2.97(m, 4H, $(CH_2)_2$), 1.82-1.78 (m, 4H, $(CH_2)_2$),1.34-1.28(m, 4H-$(CH_2)_2$, 1.25-1.23(m, 46H, $(CH_2)_{22}$ & ß-CH_2-spacer), 0.88-0.83(t, $(CH_3)_2$).

Methods

Nuclear Magnetic Resonance (NMR): ^{1}H NMR spectra were recorded using a Bruker Avance 300MHz spectrometer at the Chemistry department in University of Waterloo. Samples were dissolved in $CDCl_3$.

Fluorescence studies: Fluorescence emission spectra of pyrenyl gemini surfactants in aqueous solutions and pyrene in methanol have been recorded using Spectra max M5 microplate reader (molecular devices, USA) at excitation wavelength 363nm. These samples were measured in transparent disposable cuvettes (ZEN0118) (Malvern instruments, UK). The excitation and emission slit-widths were set at 1 nm. An average of 40–50 scans was recorded.

CMC determination: The CMC of each surfactant was determined using both surface tension and specific conductance techniques. Surface tension measurements were performed using a Lauda TE3 automated tensiometer (Lauda,

View Article Online
DOI: 10.1039/C6CP07688B

Germany), applying the Du Nuoy ring method. The Harkins and Jordan correction factor was applied to all surface tension values.[12] 40 mL of milli-Q quality water was placed in a 100 mL vessel and a concentrated (approximately 5 times of the CMC based on the pyr-3-12) sample of aqueous surfactant solution was titrated into this. Surface tensions were measured until the variability between measurements was less than 0.1 mN/m. All CMC determinations were carried out in duplicate at temperatures of 25°C.

The specific conductivities were determined with a SevenEasy™S30 conductivity meter (Mettler Toledo, Switzerland) and double-walled glass titration cell (Fisher Scientific, USA). A cell constant of 0.56cm^{-1} was determined for the conductivity probe. Again, a concentrated surfactant solution was titrated into XX mL of milli-Q water contained in the titration cell, and the CMC was again determined in duplicate at temperatures of 25, 30, and 35°C. The CMC value was determined from the abscissa of the inter-section of the trend lines connecting the experimental points before and after the CMC (observed as a clear break between two linear regions) in a surface tension vs. log concentration plot.[13] The conductivity vs concentration data was fit to Equation 1 according to the method of Carpena et al.: [14]

$$\kappa = \kappa^{o} + A_1 C + d(A_2 - A_1) ln\left(\frac{1+e^{(C-CMC)/d}}{1-e^{(-CMC)/d}}\right) \quad [1]$$

where κ^{o} and κ are the initial and solution conductivities (respectively), C is the solution concentration, A_1 and A_2 are the pre and post CMC slopes of the conductivity vs concentration curve, and d is the width of the transition region.[15]

Krafft Temperature: The Krafft temperature and Krafft point (T_k) for each surfactant were determined by the specific conductivity method as previously reported.[16] The temperature was controlled with a RE304 circulating water bath (Lauda, Germany).

Molecular Modeling: Molecular docking studies for pyrene based surfactants were performed to give additional information on how pyrenyl surfactants interact with each other (either via self and/or intermolecular aggregation) when present in the aqueous phase.[17] Discovery Studio (DS) Structure-Based-Design software (version 4.5, BIOVIA, San Diego, U.S.A) was used for the docking studies. Briefly, 3D models of the pyrene based surfactants (surrounded with water molecules) were built using the Build Fragment tool. Energy minimization was performed using the steepest descent and conjugate gradient minimizations for 1000 interactions. The distance dependent dieletric model was used as the implicit solvent model for the energy minimization step. The CDOCKER algorithm was used to dock a surfactant monomer with another monomer after defining a 25Å sphere radius around the surfactant molecule. The CHARMm force field was used for the docking studies. The most stable binding models between the pyrene based surfactants was evaluated based on CDOCKER energy and CDOCKER interaction energy in Kcal/mol. The type of interaction occurring between the Interacting pyrene surfactants (i.e. self or intermolecular).

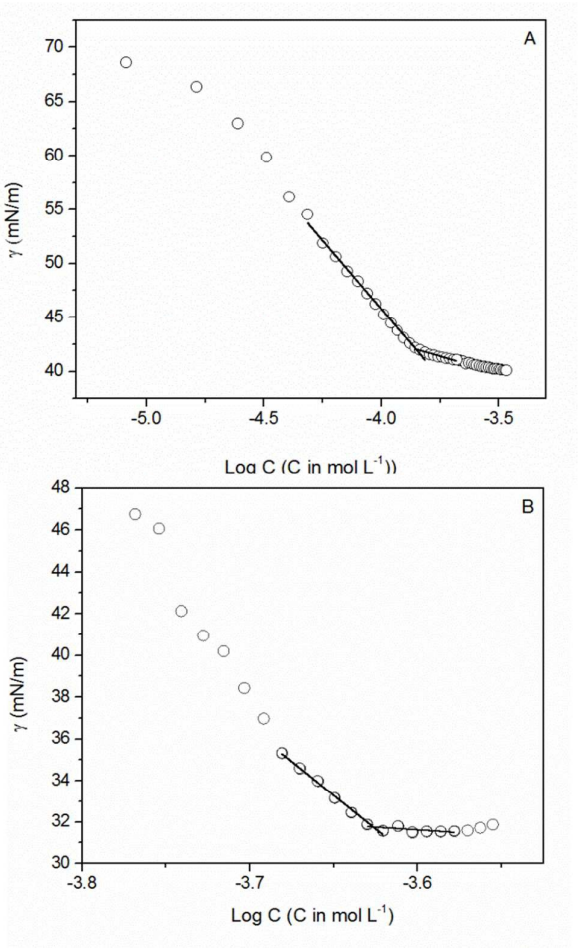

Fig. 1: Surface tension plots for A) pyrenyl-substituted gemini surfactants; Pyrene-3-14 (○) B) dissymmetric 12-3-n gemini surfactants 12-3-16. All measurements were made at 25°C. The point of intersection of the linear regions of the curves corresponds to the CMC, tabulated in Table 1.

Results and Discussion

Surface tension plots for of the pyr-3-n and 12-3-n gemini surfactants are shown in Fig.1A & 1B and the CMC values are listed in table 1.Figure 1A and 1B, respectively. The CMC values were determined from the point of intersection of the two linear regions of the γ vs. log C curves, and are tabulated in Table 1. It can be seen that the CMC gradually decreases with an increase in the length of the alkyl tail from octyl to octadecyl, for both the alkyl and pyrenyl dissymmetric surfactants. In a logarithmic plot of the CMC as a function of the hydrocarbon tail, shown in Fig.2 the symmetrical m-3-m gemini surfactants show a linear pattern decrease with increasing tail length (with the exception of (18-3-18)[14],[18] , consistent with the typical behavior of surfactant molecules. When the CMCs of the pyrenyl substituted dissymmetric surfactants are plotted in this manner, they no longer exhibit a

View Article Online
DOI: 10.1039/C6CP07688B

Table (1): Critical micelle concentration (CMC), head group area (a_o), packing parameter (P), and the degree of micelle ionization (α)

Gemini surfactant	CMC (mM)[a]	CMC (mM)[b]	γ_{cmc}(mN/m)	Γ(mol/m^2)*10^{-6}	a_0 (m^2/mol)	P	α
Pyrene-3-8	0.178 ±0.02	0.13±0.007*	27.6±0.14	9.47x10^{-7}±0.07	0.35	<1	0. 42±0.01
Pyrene-3-12	0.21±0.02	0.16±0.007	43.1±0.02	2.97±0.02	0.56	1	0.61±0.00
Pyrene-3-14	0.15±0.03	0.16±0.028	41.2±0.14	1.47±0.14	1.13	0.46	0.67±0.02
Pyrene-3-16	0.14±0.03	0.132±0.0028	43.6±0.07	3.16±0.07	0.53	0.91	0.61±0.02
Pyrene-3-18	0.02±0.07	0.06±0.014	40.0±0.00	2.38± 0.00	0.70	0.65	0.57±0.01
12-3-14	0.32±0.01	0.34±0.07	26.2±0.07	5.74±0.07	0.30	<1	0.28±0.00
12-3-16	0.22±0.01	0.18±0.02	32.2±0.07	8.07±0.07	0.21	<1	0.39±0.02
12-3-18	0.17±0.02	0.18±0.02	40.2±0.14	8.68±0.14	0.19	<1	0.44±0.02
12-3-12	0.98±0.04	0.98±0.04[2]			1.11	0.38	0.23

[a] from surface tension, [b] from specific conductivity , data obtained at 25C°. *CMC break point in pyr-3-8 conductivity study was not clear.

linear behavior, but rather show a slight decrease from pyr-3-12 (0.21mM) to pyr-3-14 (0.15mM) then pyr-3-16 (0.113m M), followed by a greater decrease between pyr-3-16 and pyr-3-18 (0.02mM). Most of the pyrenyl gemini surfactants show a clear break point at the CMC. ; However, with the exception of pyr-3-18 where the CMC was poorly defined, suggesting the presence of premicellar aggregation, and this is consistent with this kind of behaviour which was previously reported before for gemini surfactants with longer alkyl tails, m<18, in 12-s-12; where s=12,14, and 20.[17]

The same behavior was reported in dissymmetric gemini surfactants with bulky unsaturated tails, such as, phytanyl-3-16 .[15] For the m-3-n surfactants, as seen in Figure 2A, the CMC of 12-3-14 was significantly less than that of 12-3-12 (0.32mM versus 0.98mM, respectively); however from n = 14 to n = 18, logCMC did not decrease in a linear fashion. It may be the case that we did not have enough data points (i.e. different dissymmetric surfactants) to identify a linear decrease for the m-3-n surfactants. An additional methylene group added to one tail in the m-3-n surfactants does have the same effect it has on the pyrenyl surfactants. However, the effect is more pronounced in the pyrenyl surfactants due to the presence of the pyrene moiety within the surfactants, which adds to the hydrophobicity of the gemini surfactant through the pyrene stacking, leading to enhanced hydrophobic interactions. The contribution of additional methylene unit to the CMC value in both groups of surfactants was more like that of a single-tail surfactant.[19] This is attributed to the increased intermolecular hydrophobic interactions between tails of same length between the monomers within the micelles. Similar to the symmetric gemini surfactants, γCMC decreases with increasing the m-3-n concentration, which indicates the formation of a monolayer at the air/water interface, which reduces the surface tension of water. For the pyrenyl surfactants, the γ values are relatively higher than those for the corresponding symmetric m-3-m and the dissymmetric m-3-n surfactants, suggesting an earlier onset of micellization (with the exception of the pyr-3-8). Pyr-3-8 has a short alkyl tail, rendering the surfactant more hydrophilic and increasing its solubility in water, favoring the bulk over the surface.

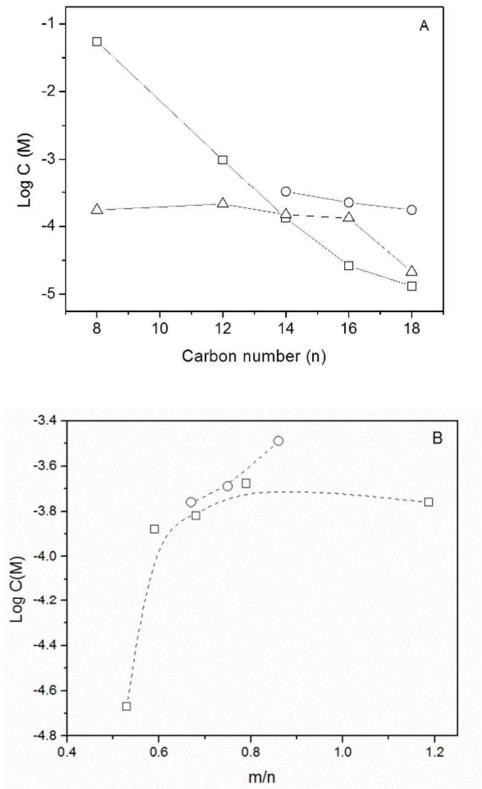

Fig. 2: Variation of the Logarithm CMC (determined by tensiometery) as a function of the alkyl tail length (A) and as a function of the degree of dissymmetry (B) for the gemini surfactants m3-m. (■), pyr-3-n (▲), 12-3-n (●).

The low value for γ_{cmc} (27.6 mN/m) is consistent with this interpretation. However, the CMC value of pyr-3-8 (0.18mM) is way lower than that of 8-3-8 symmetric counterpart (57mM).[20] The CMC value of pyr-3-8 is also lower than that of pyr-3-12. This can be attributed to the length of the hexyl pyrenyl tail which is equal to 11-11.5 bonds and this makes pyr-3-12 acts as symmetrical gemini surfactants below the CMC, thus minimize the effect of the intermolecular hydrophobic interactions, limiting the pi-pi stacking and enhancing the interactions with the dodecyl tail.

View Article Online
DOI: 10.1039/C6CP07688B

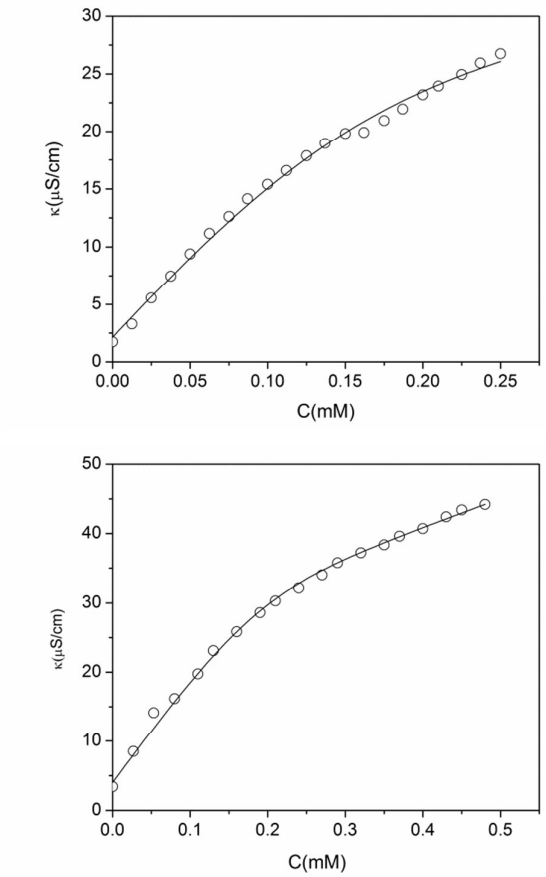

Fig. 3: A) Specific conductance (κ) versus Surfactant concentration for pyr-3-14(○) and 12-3-14(○), respectively.

The CMCs for pyr-3-12, pyr-3-14, and pyr-3-16 obtained from the conductivity studies are in good in agreement with those obtained from tensiometry, as well as with those reported previously in the literature. [5] Less agreement was observed for pyr-3-18,which is common when comparing the results using different techniques to measure different properties in self-assembly[5, 21]; particularly for surfactants having very low CMC values. CMCs for 12-3-14, 12-3-16, and 12-3-18 were also in good agreement with those obtained from the surface tension measurements. The degrees of micelle ionization parameter (α) is defined as a fraction of an ionic surfactant's counter ions that are dissociated from micelles, leaving the micelles charged, and it can be obtained from the ratio of A2/A1.[22] For both the pyrenyl and the 12-3-n gemini surfactants, α values are higher for the pyrenyl surfactants compared to the m-3-m surfactants, despite having low CMC values. Higher α values correspond to a greater degree of dissociation of the counterions from the surface of the micelles. With higher α, the repulsive forces between the partially charged micelles will play greater role in the aggregate structures within the micelles. The pyrenyl surfactants also exhibit a strong upward curvature in the plot of κ vs. C in the region of the CMC, which is an indication of the formation of premicellar aggregates.[23] Similar behaviour was observed for the 12-3-n surfactants. The CMC values decreased with the increase of the alkyl tails, and the increase in the temperature (in the supplementary data). The decrease in the CMC with the increase in the temperature is a consequence of the decreased hydrophilicity of the surfactants molecules and this reduction of hydration favors micellization. Also, the increase in temperature breaks down the structured water surrounding the hydrophobic groups.[24]

The minimum head group areas for gemini surfactants are also reported in Table. 1. The head group areas can be calculated from the surface excess concentration according to equation 2 below:

$$a_0 = (N_A\Gamma)^{-1} \quad [2]$$

where N_A is Avogadro's, and Γ is the surface excess concentration calculated from the Gibb`s adsorption equation[25]:

$$\Gamma = \frac{-1}{2.303RT}\left(\frac{d\gamma}{d\log C}\right) \quad [3]$$

where R is the gas constant, T is the absolute temperature in Kelvin, γ is the surface tension in mN.m^{-1}, ($d\gamma/d\log C$) is the slope of the linear part of the γ-logC plot and n = 3 for gemini surfactants, accounting for 1 dimeric ion and 2 monomeric counter ions. The head group areas (a_0) for the pyrenyl gemini surfactants are all smaller than that of their symmetrical counterparts with the exception of pyr-3-14 with 1.13nm^2·mol^{-1}.[5] Increased asymmetry, enhances the hydrophobic intermolecular interactions, leading to lower CMC values and higher aggregation ability.[7] Also, with longer hydrocarbon tails, a_o values decrease due to higher packing density at the air/water interface in comparison to their symmetrical counterparts. For pyr-3-18, although a_0 is higher than pyr-3-16, it is still lower than that of its symmetrical counterpart 18-3-18 which has a value of 1.28nm^2·mol^{-1},[18]. Similarly, a_0 for pyr-3-14 is lower than that of 14-3-14 (1.35nm^2·mol^{-1}) .[26, 27]

The variations in head group areas for the m-3-n surfactants result from differences in the packing of the hydrophobic tails at the air/water interface. The a_0 values for the m-3-n surfactants are lower than those for their symmetrical m-3-m counter parts, which suggests increased packing at the air/water interface as a result of the dissymmetry between the alkyl tails. A trend was established for 12-3-n surfactants. For 12-3-14, 12-3-16, and 12-3-18, a_0 values are smaller than the a_0 values of their symmetrical counterpart. As the hydrophobicity of the 12-3-n surfactants increase, the CMC values decrease, and the surfactant monomers favour adsorption at the air/water interface. This

View Article Online
DOI: 10.1039/C6CP07688B

Table (2): Critical micelle concentration (CMC), head group area (a_s), packing parameter (P), and the degree of micelle ionization (α)

T (^oK)	Surfactant	Krafft temperature (T_K)	CMC (mM)[a]	ΔG^o_m(kJ mol^{-1})	ΔH^o_m(kJ mol^{-1})	ΔS^o_m(kJ K^{-1} mol^{-1})	$T\Delta S^o_m$(kJ mol^{-1})
	Pyrene-3-8	20	0.13	-49	35	0.28	84
	Pyrene-3-12	42	0.16	-56	17	0.25	74
	Pyrene-3-14	45	0.15	-53	81	0.45	134
	Pyrene-3-16	60	0.13	-57	28	0.28	85
298.15	Pyrene-3-18	<60	0.06	-64	32	0.32	96
	12-3-14	33	0.34	-73	29	0.34	101
	12-3-16	35	0.18	-70	3.5	0.24	73
	12-3-18	60	0.18	-66	8.6	0.25	75
	12-3-12		0.98	-70	-	-	-
303.15	Pyrene-3-8		0.12	-51	36	0.29	87
	Pyrene-3-12		0.16	-46.	18	0.21	64
	Pyrene-3-14		0.075	-65	84	0.49	149
	Pyrene-3-16		0.12	-47	28	0.25	75
	Pyrene-3-18		0.042	-69	33	0.33	102
	12-3-14		0.25	-70	30	0.32	99
	12-3-16		0.18	-65	3.7	0.23	69
	12-3-18		0.18	-64	8.6	0.24	73
308.15	Pyrene-3-8		0.10	-52	37	0.29	89
	Pyrene-3-12		0.12	-51	18	0.23	69
	Pyrene-3-14		0.05	-67	87	0.5	154
	Pyrene-3-16		0.09	-61	29	0.29	90
	Pyrene-3-18		0.039	-61	34	0.31	95
	12-3-14		0.23	-67	31	0.31	97
	12-3-16		0.17	-69	3.7	0.24	73
	12-3-18		0.16	-68	8.9	0.25	77

[a] from specific conductivity.

leads to a higher degree of intermolecular interactions between the alkyl tails, resulting in smaller mean molecular area. However, the discrepancy found in the pyrenyl gemini surfactants was reported in other surfactants, such: phytanyl-3-m by Wang et al. The head group areas for both of phy-3-12, and phy-3-16 surfactants were smaller than those of 12-3-12, and 16-3-16 surfactants (phy-3-12=0.78nm^2.mol^{-1}, phy-3-16-0.91nm^2.mol^{-1}), respectively.[21] However, phy-3-18 was approximately 1.5 times that of 18-3-18 (phy-3-18=1.92nm^2.mol^{-1}) .[28]

The packing parameter, P, of a surfactant describes the shape of the aggregates formed by the surfactant in aqueous solution, and can be calculated from:

$$P = v/a_0 \times l \qquad [4]$$

where v is the hydrophobic volume of a surfactant molecule (calculated from Tanford's equations[29]):

$$v = 0.0274 + 0.0269n \quad [5]$$

and l is the length of the hydrocarbon tails (also calculated from Tanford's equations[29]):

$$l = 0.154 + 0.1265n \quad [6]$$

In equations 5 and 6, n is the number of carbon atoms in the hydrocarbon tails of the surfactant. The packing parameter for the py-3-m surfactants is dramatically impacted by the presence of the bulky pyrenyl ring in the molecule. The calculated values of the volume, length, and the packing parameter for the py-3-n are reported in Table 2. The total volume of the hydrophobic tails is given by (v_1 + v_2) and the length of the hydrophobic group will be equal to the length of the longest tail. As seen in Table 2, as well as in the literature, aggregates formed by m-3-m gemini surfactants tend to form cylindrical micelles with a P value of approximately 0.35 depending upon the alkyl tail length. The replacement of one of the tail group by a pyrenyl ring dramatically impacts the hydrophobic volume due to the bulkiness of the fused rings without impacting the overall length of the hydrophobic group except for the py-3-8 surfactant. This restricts the geometry of the system such that cylindrical, lamellar and inverted micelles are now the predicted favorable geometry.

These different packing values are affected by the head group area as well. The head group areas of the pyrenyl surfactants showed no consistency whatsoever in the data obtained from the surface tension. In equations 5 and 6, n is the number of carbon atoms in the hydrocarbon tails of the surfactant. The packing parameter for the pyrene-3-n gemini surfactants is dramatically impacted by the presence of the bulky pyrenyl ring in the molecule. The aggregates shapes predicted by equation 4 are cylindrical (pyr-3-14), vesicles (pyr-

View Article Online
DOI: 10.1039/C6CP07688B

3-16), inverted micelles (pyr-3-8), or lamellar (pyr-3-12 and pyr-3-18). This may be due to the presence of the bulky pyrene ring which adds to the hydrophobic volume, but not to the length of the tail.[21] For 12-3-n surfactants, inverted micelles were formed. This is largely due to the small head group areas that were caused by tight packing at the air/water interface as a result of increased intermolecular hydrophobic interactions between the alkyl tails.

Pyrenyl and 12-3-n gemini surfactants behave similarly when measuring the Krafft temperatures. However, at higher temperatures there was a second break point and we believe it indicates a phase transition and the beginning of the formation of higher and more complicated morphologies. The values of the Krafft temperatures and the transition temperatures of the eight surfactants were obtained from the plots of the temperature- specific conductance and are presented in Table 2 and Figure 4.

The thermodynamic parameters of micelle formation for the py-3-n and the 12-3-n gemini surfactants were calculated by applying the pseudo-phase separation model for ionic surfactants according to[30]:

$$\Delta G^{o}_{m} = 2(1.5-\alpha)RT\ln X_{cmc} \quad [7]$$

$$\Delta H^{o}_{m} = -RT^{2} x\, \delta \ln_{cmc}/\delta T \quad [8]$$

$$\Delta S^{o}_{m} = \Delta H^{o}_{m} - \Delta G^{o}_{m} / \delta T \quad [9]$$

where α is the degree of micelle ionization, which was obtained from the conductance titrations, and X_{cmc} is the molar fraction at the CMC, X_{cmc}= CMC/55.4, the fact that 1 L of water corresponds to 55.4 mol of water at 25°C is responsible for the value of 55.4, CMC is in mol·L^{-1}.

The thermodynamic parameters of micelle formation are listed in Table 2 for both the py-3-n and 12-3-n series of surfactants different temperatures. As the solution decrease, corresponding to ΔG^{o}_{m} becoming more negative, and micelle formation becoming more spontaneous. For the pyrenyl surfactants, the results show that at a certain temperature, as the m/n ratio increases, ΔG^{o}_{m} values become more negative

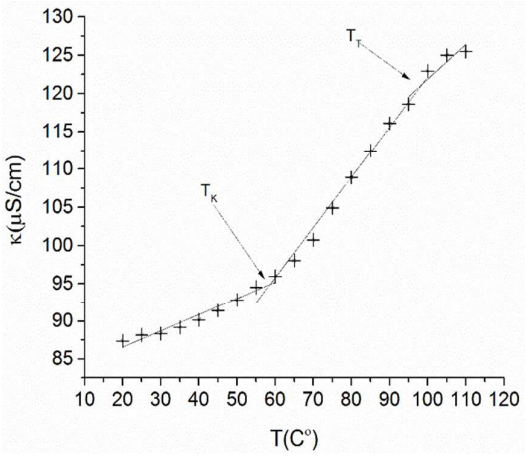

Fig 4: Krafft point (T_K) determination for the 12-3-16 gemini surfactant.

and this implies the spontaneity of the aggregation process, also ΔG^{o}_{m} increases for the same surfactant at different temperatures, which lead to lower CMC. The higher the temperature, the lower the CMC with the increased hydrophobicity as a result of increased alkyl tail length. However, the process of micellization is entropy driven as ΔH^{o}_{m} is positive throughout the pyrenyl and the dissymmetrical surfactants as well and this means that the removal of a surfactant tail from the water into the core is endothermic. In the dissymmetrical gemini surfactants ΔG^{o}_{m} values were decreasing from 12-3-14 to 12-3-18 at a specific temperature, which suggests that the addition of one methylene unit to one tail is endothermic and requires more energy relative to the pyrenyl and to the symmetrical counterparts gemini surfactants. This might be attributed to the increase in the disorder of the solution, leading to a decrease in ΔG^{o}_{m}. This was confirmed by the plot of the variation of (ΔG^{o}_{m} (CH_2)) with the degree of dissymmetry m/n, which shows the relationship between the Gibbs free energy per mole of CH_2 (ΔG^{o}_{m} (CH_2)) with the degree of the dissymmetry (see Fig.5). In the pyrenyl surfactants, as the m/n increases, the ΔG^{o}_{m} becomes more negative, which favors the aggregation led by the hydrophobic interactions. Values of $|T\Delta S^{o}_{m}|$ for all of the asymmetric gemini surfactants in this study were higher than those of $|\Delta H^{o}_{m}|$, which again suggests that the aggregation process of these surfactants is entropy-driven.[31] However, when comparing the dissymmetric gemini surfactants to the pyrenyl surfactants, we notice that ΔG^{o}_{m} of 12-3-14>pyr-3-14, 12-3-16>pyr-3-16, and 12-3-18>pyr-3-18 at the same temperature, although the latter`s difference is not that significant as those of 12-3-14 and 12-3-16. This suggests that substituting an alkyl tail with hexyl pyrene increases the entropy and becomes less spontaneous relative to the symmetrical and to the 12-3-n gemini surfactants. This is probably due to the geometric restraints created by the aromatic pyrene.

Pyrene has been widely used as a fluorescent probe to characterize micro-heterogeneous systems, such as; micelles.[32] This is largely due to the significant sensitivity to the polarity of the solvent being used. Pyrene shows several characteristic vibronic bands in the region of 370 – 400 nm in its fluorescence emission spectrum. The absolute and relative intensities, and the width and position of these bands depend highly on the polarity of the microenvironment. [33]Due to the low solubility of pyrene in pure water, the efficiency of excimer formation is low at surfactant concentrations below the CMC. At concentrations greater than the CMC, pyrene molecules will be crowded into the micelles, resulting in excimer formation and the appearance of a broad excimer emission band near 500 nm.[34] In this study, for the py-3-m surfactants, pyrene is part of the structure of the surfactants molecules themselves. At concentrations below the CMC, formation of pre-micellar aggregates, known to commonly occur, particularly for more hydrophobic gemini surfactants, could result in the appearance of excimer emission. The emission spectra for the py-3m surfactants (see Fig. 6) in water

View Article Online
DOI: 10.1039/C6CP07688B

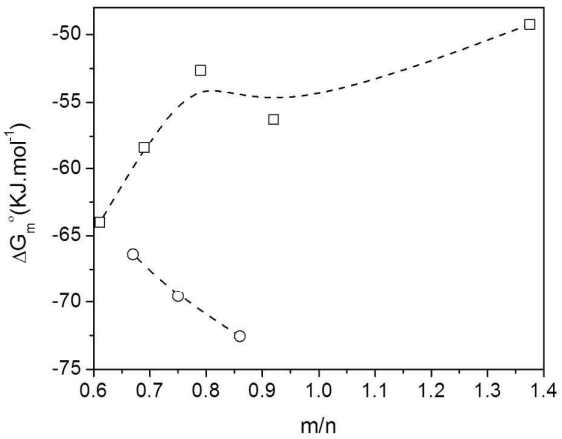

Fig.5 The variation of ($\Delta G^{o}_{m}(CH_2)$) with the degree of dissymmetry m/n at 25ºC from the conductivity studies for Pyr-3-n (■), and 12-3-n (●).

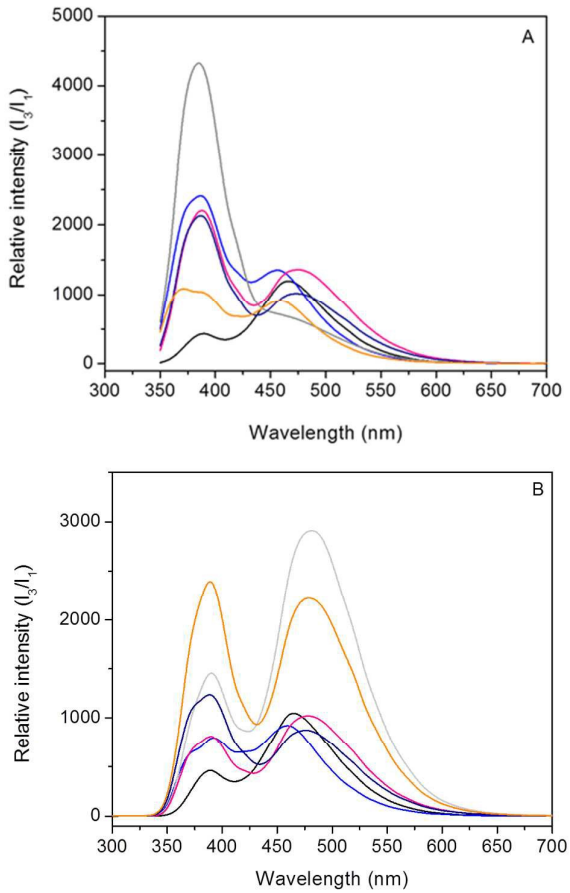

Fig.6: Fluorescence spectra of pyrenyl gemini surfactants, a) before the CMC (0.01mM). b) Post the CMC (0.5mM). (Pyrene black, pyr-3-8 blue, pyr-3-12 grey, pyr-3-14 pink, pyr-3-16 navy, and pyr-3-18 orange), a) before the CMC. b) Post the CMC. The intensity of the excimer peak in pre-CMC solution is lower than the intensity of the peak after the CMC, which indicates the presence of the pyrene with in the hydrophobic micelles.

both below (Fig. 6A) and above (Fig. 6B) the CMC are comparable to the spectrum obtained for pyrene in methanol with monomer fluorescence maxima at 390nm that are well resolved from a broad peak in the range of 450–500 nm (data not shown), resulting from excimer formation. A small red shift for the excimer peak was observed of the py-3-m surfactants (as compared to pyrene alone) and is most likely the effect of increased hydrophobicity environment around the pyrene group caused by the formation of the micelles. In Fig. 6A, excimer formation can be observed at surfactant concentrations below the CMC (0.01mM) for all of the surfactants except pyr-3-12, indicating an evidence for the formation of premicellar aggregates possibly due to increased association of the tail groups of adjacent surfactant molecules through possible pi-pi interactions.

To further explore the nature of the interaction(s) between the tail groups of the py-3-m surfactants, docking simulations were carried out. The docked poses (see Figure 7) obtained were ranked based on CDOCKER energy and CDOCKER interaction energies in kcal mol^{-1} and the type of polar and nonpolar interactions observed between the surfactant were analysed. The results of these studies indicate that the intermolecular pi-pi stacking interactions between pyrene rings on adjacent py-3-8 surfactant molecules was the most favoured type of interaction occurring between the molecules (Figure 7A). It was also observed that intermolecular and pi-sigma stacking interactions occurred (Figure 7B) and these interactions actually gave the most stable bimolecular complex (Fig. 7B). Similar results were obtained for each of the py-3-m surfactants, although the tendency for self-aggregation within a single surfactant molecule increases as the alkyl chain length increases, as in the case of Pyr-3-18, where very strong intramolecular cation-pi and pi-sigma interactions were observed (Fig.7C).

Conclusions

The pyrene-based gemini surfactants, pyr-3-n, (n=8, 12, 14, 16, and 18), and the dissymmetric gemini surfactants, 12-3-n, n = (14, 16, 18) were synthesized and their aggregation properties were characterized. The Krafft temperatures of pyrene-3-n and 12-3-n increased with the increase in the alkyl tail length. This finding following the general observations with all other gemini surfactants. Pyr-3-n and 12-3-n showed much lower CMC values than those of their symmetrical counterparts, confirming previous findings with pyr-3-12[10], and those of *m-6-n* reported by Wang *et al.*.[31] The low CMC values are due to increased hydrophobicity of the pyrene-3-n surfactants, and due to the dissymmetry of the 12-3-n gemini surfactants, which imparts unique properties on the surfactants. The docking studies showed that the first interaction happening in the pyr-3-n surfactants is the pyrene-pyrene interactions (through pi-pi stacking), and this may cause the initiation of the micelle formation starting at a very high surface tension. The pyrene in here is included as a guest molecule into the micelle and this is due to the high hydrophobicity of the pyrene molecules, driving them to prefer the micelle core. Self-aggregation behaviour was also associated with increased length of the alkyl tail, which gave unique and diverse

View Article Online
DOI: 10.1039/C6CP07688B

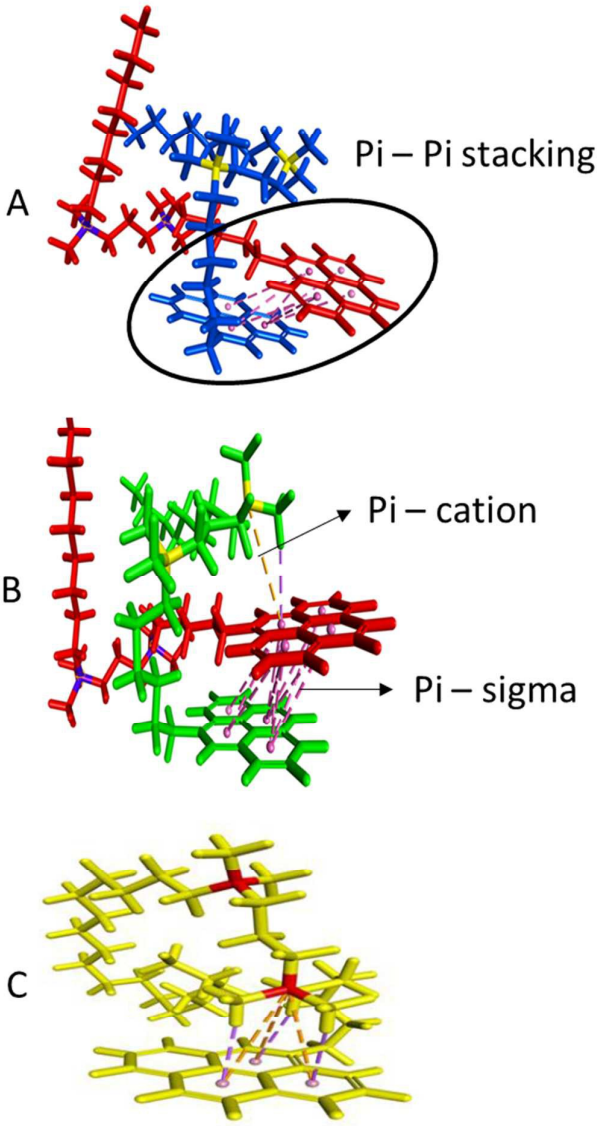

Fig. 7. A) Intermolecular pi-pi interactions (purple line) between the two pyr-3-8 surfactants. B) Intermolecular pi-cation (yellow line) and pi-sigma (purple line) interactions between the two pyr-3-8 surfactants. C) Intramolecular pi-cation (orange line) and pi-sigma (purple line) interactions in the interactions in the pyr-3-18 surfactant.

morphological structures in solution. Higher degrees of micellization were also observed in both of the groups, the pyrenyl surfactants and the dissymmetric ones. The higher the α value, the easier the binding of the DNA to the surfactants as it replaces the counterions to reduce the repulsive attraction forces between the two head groups. This behaviour is what makes these surfactants attractive to be employed as a possible transfection vectors. This property was confirmed by Wang et al. in the phyanyl gemini surfactants, which gave higher transfection efficacies than the other symmetrical ones.[35] Head group areas are smaller in pyrene-based surfactants than those of the symmetrical counterparts, indicating enhanced intermolecular hydrophobic interaction, which results in smaller a_o. However, pyrene-3-14 has a relatively larger head group area. This may be caused by the dissymmetry effect appearing at this surfactant, because before that pyr-3-12 is close to symmetry and pyr-3-8 has very low surface tension due to their high solubility in aqueous phase. The packing parameter is calculated for the pyr-3-n and 12-3-n compounds are indicative of the formation of various morphologies, especially in the pyr-3-n surfactants. Pyr-3-8 forms inverted micelles, whereas pyr-3-14 forms spherical micelles, pyr-3-12 and pyr-3-18 form lamellar micelles, and pyr-3-16 forms vesicles. Both vesicles and inverted micelles have been linked to better transfection results in the literature. Pyr-3-12 reacted differently from the rest of the pyrenyl surfactants and again this can be attributed to its unique structure, which caused it to have more negative ΔG^o_m at 25°C than pyr-3-14. All of the dissymmetric gemini surfactants in this study showed that the micellization process is entropy driven, which resonates with Wang *et al*. findings with *m-6-n,* and that the dissymmetry and the length of the tail require more energy contribution in order to initiate the micellization process.

Acknowledgements

The authors would like to thank The Saudi Cultural Bureau and the Ministry of higher education for the financial funding provided as part of the Scholarship program of the late King Abdullah Bin AbdulAziz Al Saud. SDW is supported by the Natural Sciences and Engineering Research Council of Canada (NSERC Discovery Grant #335626-2011). The School of Pharmacy, University of Waterloo is gratefully acknowledged for providing access to the core equipment facility used in this research.

Notes and references

1. A. J. Kirby, et al., *Angew Chem Int Ed* 2003. **42**, 1448.
2. S. D. Wettig, R.E.Verall, M. Foldvari, *Curr gene ther*, 2008. **8**: p. 9.
3. M.J. Rosen, D.J. Tracy, *J.Surfactant Deterg.*, 1998. **1**, 547.
4. R. Zana, Adv. *Colloid Interface Sci.*, 2002. **97**, 205.
5. Y. Fan, Y. Li, M. Cao, J. Wang, Y. Wang, R.K. Thomas, *Langmuir*, 2007. **23**,11458.
6. R.Zana, *J. Colloid Interface Sci.,* 2002. **248**, 203.
7. R. Oda, S.J. Candau, I. Huc, *Chem. Commun.*, 1997. **21,** 2105.
8. M. Sikirić, I. Primožič,Y. Talmon, N. Filipović-Vinceković, *J. Colloid Interface Sci.*, 2005. **281**, 473.
9. G. Bae, J, Wang, Y, Wang, H, Yan, R .K, Thomas, *J. Phys.Chem. B,* 2002. **106**, 6614.
10. C. Wang, S.D. Wettig, M. Foldvari, R.E. Verrall, *Langmuir*, 2007. **23**, 8995.
11. F. Nakamura, M. Hara, *Mol.Cryst. Liq. Cryst.,* 2002. **377**, 57.

View Article Online
DOI: 10.1039/C6CP07688B

12. W.D. Harkins, H.F. Jordan, *J.Am. Chem.Soc,* 1930. **52**, 1751.
13. E. Fisicaro, C. Compari, E. Duce, M. Biemmi, M. Peroni, A. Braibanti, *Phys.Chem.Chem. Phys.*, 2008. **10**, 3903.
14. P. Carpena, J.Aguiar, P. Bernaola-Galván,C. Carnero Ruiz, *Langmuir*, 2002. **18**, 6054.
15. H. Wang, S.D. Wettig, *Phys. Chem. Chem. Phys.*, 2011. **13**, 637.
16. A.Z. La nergne, Y. Zhu, A. Pizzino, V. Molinier, J.M. Aubry, *J. Colloids Interface Sci.*, 2011. **04**, 9.
17. E. Fisicaro, C. Compari, F. Bacciottini, L. Contardi, N. Barbero, G. Viscardi, P. Quagliotto, G. Donofrio, B. Różycka-Roszak, P. Misiak, E. Woźniak, F. Sansone, *J. Phys. Chem. B,* 2014, **118**, 13183.
18. Q. Chen, D.Zhang, R. Li, H. Liu, Y. Hu, *Thin Solid Films,* 2008. **516**, 8782.
19. X. Wang, Q. Li, X. Chen, Z. Li, *Langmuir,* 2012. **28**: p. 16547.
20. M. Frindi, B. Michels, H. Levy, R. Zana, *Langmuir*, 1994. **10**, 1140.
21. H. Wang, , S.D. Wettig, *Phys. Chem. Chem. Phys.*, 2011. **13**, 637-642.
22. B. L. Bales, *J.Phys. Chem.B*, 2001. **105**,6798.
23. X, Li, S.D. Wettig, C. Wang, M. Foldvari, R.E. Verrall,, *Phys.Chem. Chem. Phys.*, 2005. **7**, 3172.
24. E. Mahmood and D.A.F. Al-Koofee, *GJSFR*, 2013. **13**.4
25. F. Devínsky, I. Lacko,F. Bittererová, L. Tomečková, *J.Colloid Interface Sci.*, 1986. **114**, 314.
26. L. Han, Z.Ye, H. Chen, P. Luo, *J.Surfactant Deterg.*, 2009. **12**, 185.
27. H. Wang, T. Kaur, N. Tavakoli, J. Joseph, S.D. Wettig, . *Phys. Chem. Chem.Phys.*, 2013. **15**, 20510.
28. R. Nagarajan, *Langmuir*, 2002. **18**, 31.
29. R. Zana, *Langmuir*, 1996. **12**,1208.
30. X. Wang, et al., J. Phys. Chem. B, 2003. **107**: p. 11428.
31. T.H. Förster, B. Selinger, *Z. Naturforsch.*, 1964. **19**,38.
32. K. Kalyanasundaram, J.K. Thomas, *J. Am. Chem. Soc.*, 1977. **99**, 2039.
34. L. Sahoo, J. Sarangi, and P.K. Misra, Bull. Chem.Soc. Jpn., 2002. **75**: p. 859.
35. H. Wang and S.D. Wettig, Phys. Chem. Chem.. Phys, 2011. **13**: p. 637.

View Article Online
DOI: 10.1039/C6CP07688B

For Table of Contents only